symmetry

Article

Timelike Circular Surfaces and Singularities in Minkowski 3-Space

Yanlin Li [1,*], Fatemah Mofarreh [2] and Rashad A. Abdel-Baky [3]

[1] School of Mathematics, Hangzhou Normal University, Hangzhou 311120, China
[2] Mathematical Science Department, Faculty of Science, Princess Nourah bint Abdulrahman University, Riyadh 11546, Saudi Arabia
[3] Department of Mathematics, Faculty of Science, University of Assiut, Assiut 71516, Egypt
* Correspondence: liyl@hznu.edu.cn

Abstract: The present paper is focused on time-like circular surfaces and singularities in Minkowski 3-space. The timelike circular surface with a constant radius could be swept out by moving a Lorentzian circle with its center while following a non-lightlike curve called the spine curve. In the present study, we have parameterized timelike circular surfaces and examined their geometric properties, such as singularities and striction curves, corresponding with those of ruled surfaces. After that, a different kind of timelike circular surface was determined and named the timelike roller coaster surface. Meanwhile, we support the results of this work with some examples.

Keywords: striction curve; ingularities; timelike roller coaster surfaces

MSC: 53A04; 53A05; 53A17

check for updates

Citation: Li, Y.; Mofarreh, F.; Abdel-Baky, R.A. Timelike Circular Surfaces and Singularities in Minkowski 3-Space. *Symmetry* **2022**, *14*, 1914. https://doi.org/10.3390/sym14091914

Academic Editor: Lorentz Jäntschi

Received: 26 July 2022
Accepted: 6 September 2022
Published: 13 September 2022

1. Introduction

In spatial kinematics, the movement of the one-parameter family of circles with stationary radius constructs a circular surface, while the movement of the one-parameter family of lines constructs a ruled surface. A circular surface has a spine curve, and a ruled surface has a striction curve. The envelope of the tangent lines to a space curve defines a tangent developable ruled surface. The characteristics of a tangent ruled surface are straight lines which are tangential to the edge of regression. The edge of regression designates singular points of the tangent developable ruled surface [1–6]. With an analogous notion for ruled surfaces, geometers have investigated circular surfaces in the Euclidean and Minkowski 3-spaces. For example, Izumiya et al. [7] discussed several geometric possessions and singularities of circular surfaces corresponding with ruled surfaces. In [8], the authors initiated great circular surfaces which were generated as a one-parameter family of great circles in three spheres, and they gained a comprehensive classification of the singularities of such surfaces while also discussing the geometric explanations via points of spherical geometry. In [9], a new denomination of circular surfaces in Euclidean 3-space was considered by a curve and a conformity of circles. The authors particularly inspected some geometrical characterizations of circular surfaces in case the base curve was an algebraic curve. Spacelike circular surfaces in Minkowski 3-space are introduced, and several geometric possessions are obtained [10]. Furthermore, the authors defined spacelike roller coaster surfaces as spacelike circular surfaces in the case when the generated circles were curvature lines. Tuncer et al. [11] defined the equations of a spacelike circular surface and spacelike roller coaster surface depending on the unit split quaternions and homothetic movements. In [12], Nadia Alluhaibi presented some new results regarding circular surfaces in Euclidean 3-space. Nadia Alluhaibi also showed the conditions for the roller coaster surfaces to be minimal surfaces or flat. In [13], R. Abdel-Baky et al. studied timelike circular surfaces in Minkowski 3-space. However, they did not consider the singularities' properties. In this work, we consider the geometrical possessions and singularity of a timelike circular surface with a stationary radius in Minkowski 3-space $\mathbb{E}_1^3$. In Section 3, we address a timelike circular surface and obtain its Gaussian and mean curvature. Then, we examine the conditions of the curve in order to form striction curves on the timelike circular surface. Then, we present a characterization of local singular points on timelike circular surfaces. In the case of every generated circle with a curvature line, except for the singular or umbilical points, a classification of such timelike circular surfaces into Lorentzian spheres, timelike canal surfaces, a special type of timelike surfaces or timelike surfaces is regularly linked the three surfaces. At the end, certain examples are given to support the idea of how to form the timelike roller coaster and timelike circular surface.

2. Basic Concepts

For this study, we begin with certain concepts that will be used later [14–16]. Suppose $\mathbb{R}^3 = \{(x_1, x_2, x_3) \ |, \ x_i \in \mathbb{R} \ (i = 1, 2, 3)\}$ is a 3-dimensional Cartesian space. For all $\boldsymbol{y} = (y_1, y_2, y_3)$ and $\boldsymbol{x} = (x_1, x_2, x_3) \in \mathbb{R}^3$, the Lorentzian scalar product of $\boldsymbol{y}$ and $\boldsymbol{x}$ is given as follows:

$$< \boldsymbol{y}, \boldsymbol{x} >= y_1 x_1 + y_2 x_2 - y_3 x_3.$$

$(\mathbb{R}^3, <,>)$ defines the Minkowski 3-space, and we use it as an alternative to $\mathbb{E}_1^3$ $(\mathbb{R}^3, <,>)$. A non-zero vector $\boldsymbol{x} \in \mathbb{E}_1^3$ defines whether it is spacelike, lightlike or timelike in the case where $< \boldsymbol{x}, \boldsymbol{x} >> 0$, $< \boldsymbol{x}, \boldsymbol{x} >= 0$ or $< \boldsymbol{x}, \boldsymbol{x} >< 0$ in the same order. The norm of $\boldsymbol{x} \in \mathbb{E}_1^3$ is $\|\boldsymbol{x}\| = \sqrt{|< \boldsymbol{x}, \boldsymbol{x} >|}$. Furthermore, for two vectors $\boldsymbol{y}$ and $\boldsymbol{x}$ the cross product $\boldsymbol{y} \times \boldsymbol{x}$ is

$$\boldsymbol{y} \times \boldsymbol{x} = \begin{vmatrix} \boldsymbol{i} & \boldsymbol{j} & -\boldsymbol{k} \\ y_1 & y_2 & y_3 \\ x_1 & x_2 & x_3 \end{vmatrix} = ((y_2 x_3 - y_3 x_2), (y_3 x_1 - y_1 x_3), -(y_1 x_2 - y_2 x_1)),$$

where $\boldsymbol{i}, \boldsymbol{j}, \boldsymbol{k}$ is the canonical basis of $\mathbb{E}_1^3$. The hyperbolic and Lorentzian unit spheres, are the following:

$$\mathbb{H}_+^2 = \left\{ \boldsymbol{x} \in \mathbb{E}_1^3 \mid \|\boldsymbol{x}\|^2 = x_1^2 + x_2^2 - x_3^2 = -1, x_1 > 0 \right\},$$

and

$$\mathbb{S}_1^2 = \left\{ \boldsymbol{x} \in \mathbb{E}_1^3 \mid \|\boldsymbol{x}\|^2 = x_1^2 + x_2^2 - x_3^2 = 1 \right\}.$$

Definition 1.

(i) *Spacelike angle: If $\boldsymbol{x}$ as well as $\boldsymbol{y}$ are spacelike vectors at $\mathbb{E}_1^3$ which span a spacelike vector subspace, then $|< \boldsymbol{x}, \boldsymbol{y} >| \leq \|\boldsymbol{x}\| \|\boldsymbol{y}\|$, and a unique real number $\vartheta \geq 0$ exists that is $< \boldsymbol{x}, \boldsymbol{y} >= \|\boldsymbol{x}\| \|\boldsymbol{y}\| \cos\vartheta$. It is named the spacelike angle between $\boldsymbol{x}$ and $\boldsymbol{y}$.*

(ii) *Central angle: If $\boldsymbol{x}$ and $\boldsymbol{y}$ are spacelike vectors at $\mathbb{E}_1^3$ which span a timelike vector subspace, then $|< \boldsymbol{x}, \boldsymbol{y} >| > \|\boldsymbol{x}\| \|\boldsymbol{y}\|$, and a unique real number $\vartheta \geq 0$ exists that is $< \boldsymbol{x}, \boldsymbol{y} >= \|\boldsymbol{x}\| \|\boldsymbol{y}\| \cosh\vartheta$. It is named the central angle between $\boldsymbol{x}$ and $\boldsymbol{y}$.*

(iii) *Lorentzian timelike angle: If $\boldsymbol{x}$ is a spacelike vector and $\boldsymbol{y}$ is a timelike vector at $\mathbb{E}_1^3$, then a unique real number $\vartheta \geq 0$ exists that is $< \boldsymbol{x}, \boldsymbol{y} >= \|\boldsymbol{x}\| \|\boldsymbol{y}\| \sinh\vartheta$. This is the Lorentzian timelike angle among $\boldsymbol{x}$ and $\boldsymbol{y}$.*

We indicate the surface M at $\mathbb{E}_1^3$ as follows:

$$M : \boldsymbol{P}(u, \theta) = (p_1(u, \theta), p_2(u, \theta), (p_3(u, \theta)), \ \ (u, \theta) \in D \subseteq \mathbb{R}^2. \tag{1}$$

Suppose $\boldsymbol{\Gamma}$ is a standard unit normal vector field on a surface M determined using $\boldsymbol{\Gamma}(u, \theta) = \boldsymbol{P}_u \times \boldsymbol{P}_\theta \|\boldsymbol{P}u \times \boldsymbol{P}_\theta\|^{-1}$, where $\boldsymbol{P}_i = \frac{\partial \boldsymbol{P}}{\partial i}$. Therefore, the first fundamental form (metric) I of the surface M is given as

$$I = g_{11} du^2 + 2 g_{12} du d\theta + g_{22} d\theta^2, \tag{2}$$

where $g_{11} =< \boldsymbol{P}_u, \boldsymbol{P}_\theta >$, $g_{12} =< \boldsymbol{P}_u, \boldsymbol{P}_\theta >$, $g_{22} =< \boldsymbol{P}_\theta, \boldsymbol{P}_\theta >$. In addition, the second fundamental form II of M will be as follows:

$$II = h_{11}du^2 + 2h_{12}dud\theta + h_{22}d\theta^2, \tag{3}$$

where $h_{11} =< \boldsymbol{P}_{uu}, \boldsymbol{\Gamma} >$, $h_{12} =< \boldsymbol{P}_{u\theta}, \boldsymbol{\Gamma} >$, $h_{22} =< \boldsymbol{P}_{\theta\theta}, \boldsymbol{\Gamma} >$. The Gaussian curvature K and the mean curvature H are

$$K(u,\theta) = \epsilon\frac{h_{11}h_{22} - h_{12}^2}{g_{11}g_{22} - g_{12}^2}, \ \ H(u,\theta) = \frac{h_{11}g_{11} - 2h_{12}g_{12} + h_{22}g_{22}}{2(g_{11}g_{22} - g_{12}^2)}, \tag{4}$$

where $< \boldsymbol{\Gamma}, \boldsymbol{\Gamma} >= \epsilon(\pm 1)$. A surface in the Minkowski 3-space $\mathbb{E}_1^3$ names a spacelike or timelike surface in case the induced metric at the surface is a positive or negative definite Riemannian metric, respectively. This is identical to stating that the normal vector on the spacelike or timelike surface is a timelike or spacelike vector, respectively [1–3].

3. Timelike Circular Surfaces

We consider the notion of timelike circular surfaces in $\mathbb{E}_1^3$. Let us have a non-null curve $\boldsymbol{\alpha} = \boldsymbol{\alpha}(u)$ as a regular curve with its tangent vectors $\boldsymbol{\alpha}'(u)$ such that $\|\boldsymbol{\alpha}'\| \neq 0$ for all $u \in I$, $' = \frac{d}{du}$ and a positive number $r > 0$, a timelike circular surface is defined as the surface which is swept out using a set of timelike circles with its center points following the curve $\boldsymbol{\alpha}$. Either circle names a generating circle, which lies on a Lorentzian plane named the circle plane. Assuming $\boldsymbol{e}_1$ indicates the timelike unit normal vector of a circle plane, and $\boldsymbol{e}_1$ is connected to all points of the spine curve $\boldsymbol{\alpha}$, when given a radius r of a generating circle, a timelike circular surface is specified using $\boldsymbol{\alpha}$ and $\boldsymbol{e}_1$. Henceforth, this work represents the derivative with respect to u with primes.

In this case, u is the arc length of the spacelike spherical curve $\boldsymbol{e}_1(u) \in \mathbb{H}_+^2$, and the unit spacelike tangent vector of $\boldsymbol{e}_1(u)$ is $\boldsymbol{e}_2 = \boldsymbol{e}_1'(u)$. We also have a spacelike unit vector $\boldsymbol{e}_3 = \boldsymbol{e}_1 \times \boldsymbol{e}_2$, and then we define an orthonormal moving frame $\{\boldsymbol{e}_1 = \boldsymbol{e}_1(u),\ \boldsymbol{e}_2 = \boldsymbol{e}_1'(u),\ \boldsymbol{e}_3 = \boldsymbol{e}_1 \times \boldsymbol{e}_2\}$ along $\boldsymbol{e}_1(u)$. This is named the Blaschke frame of the spherical curve $\boldsymbol{e}_1(u) \in \mathbb{H}_+^2$. It is clear that

$$\begin{gathered} - < \boldsymbol{e}_1, \boldsymbol{e}_1 >=< \boldsymbol{e}_3, \boldsymbol{e}_3 >=< \boldsymbol{e}_2, \boldsymbol{e}_2 >= 1, \\ \boldsymbol{e}_1 \times \boldsymbol{e}_2 = \boldsymbol{e}_3,\ \boldsymbol{e}_3 \times \boldsymbol{e}_1 = \boldsymbol{e}_2,\ \boldsymbol{e}_2 \times \boldsymbol{e}_3 = -\boldsymbol{e}_1. \end{gathered} \tag{5}$$

Therefore, we have the following Blaschke formulae:

$$\begin{pmatrix} \boldsymbol{e}_1' \\ \boldsymbol{e}_2' \\ \boldsymbol{e}_3' \end{pmatrix} = \begin{pmatrix} 0 & 1 & 0 \\ 1 & 0 & \gamma(u) \\ 0 & -\gamma(u) & 0 \end{pmatrix} \begin{pmatrix} \boldsymbol{e}_1 \\ \boldsymbol{e}_2 \\ \boldsymbol{e}_3 \end{pmatrix}; \tag{6}$$

where $\gamma(u)$ is the spherical or geodesic curvature of $\boldsymbol{e}_1(u) \in \mathbb{H}_+^2$. Let us express the tangent vector $\boldsymbol{\alpha}'$ as

$$\boldsymbol{\alpha}'(u) = \delta\boldsymbol{e}_1 + \sigma\boldsymbol{e}_2 + \eta\boldsymbol{e}_3, \tag{7}$$

where $\delta(u)$, $\sigma(u)$ and $\eta(u)$ define its coordinate functions. Suppose $\boldsymbol{e}_2$ and $\boldsymbol{e}_3$ construct the basis of the corresponding circle plane at all points of the spine curve $\boldsymbol{\alpha}(u)$. Therefore, for a sufficient small parameter $r > 0$, and using the solutions of the differential system in Equation (6), the timelike circular surface M is constructed as follows:

$$M : \boldsymbol{P}(u,\theta) = \boldsymbol{\alpha}(u) + r(\cos\theta\boldsymbol{e}_2(u) + \sin\theta\boldsymbol{e}_3(u)),\ u \in I,\ \theta \in \mathbb{R}. \tag{8}$$

We call $\boldsymbol{\alpha}(u)$ a spine curve, and $\theta \to \boldsymbol{\alpha}(u) + r(\cos\theta\boldsymbol{e}_2(u) + \sin\theta\boldsymbol{e}_3(u))$ is named a generating circle (Figure 1) [6]. $\gamma(u)$, $\delta(u)$, $\sigma(u)$ and $\eta(u)$ define a complete system of curvature functions (invariants) of the surface M.

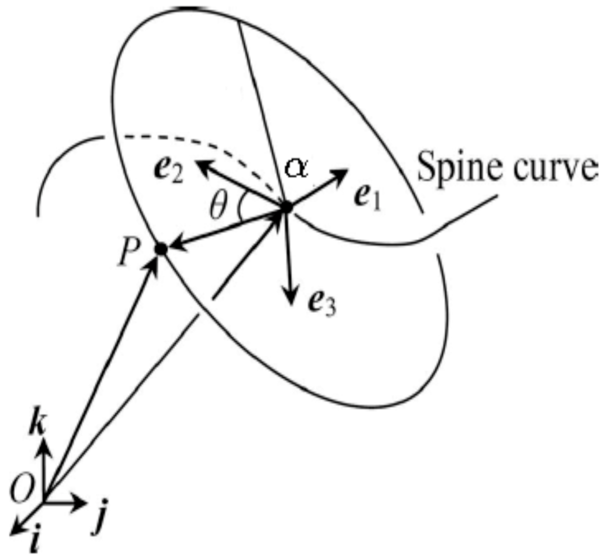

Figure 1. A cross-section of M.

In this paper, we do not consider timelike circular surfaces with fixed vectors $\boldsymbol{e}_1$. Clearly, Equation (8) gives a method for constructing timelike circular surfaces with a radius $r > 0$ by the following equation:

$$\boldsymbol{\alpha}(u) = \boldsymbol{\alpha}_0 + \left(\int_0^u \delta \boldsymbol{e}_1 + \sigma \boldsymbol{e}_2 + \eta \boldsymbol{e}_3 \right) du. \tag{9}$$

The $\boldsymbol{P}'s$ tangent vectors are

$$\left. \begin{array}{l} \boldsymbol{P}_u = (r\cos\theta + \delta)\boldsymbol{e}_1 + (\sigma - r\gamma\sin\theta)\boldsymbol{e}_2 + (\eta + r\gamma\cos\theta)\boldsymbol{e}_3, \\ \boldsymbol{P}_\theta = r(-\sin\theta \boldsymbol{e}_2 + \cos\theta \boldsymbol{e}_3). \end{array} \right\} \tag{10}$$

Then, we have

$$\left. \begin{array}{l} g_{11} = -(r\cos\theta + \delta)^2 + (\sigma - r\gamma\sin\theta)^2 + (\eta + r\gamma\cos\theta)^2, \\ g_{12} = r(r\gamma - \sigma\sin\theta + \eta\cos\theta),\ g_{22} = r^2. \end{array} \right\} \tag{11}$$

The spacelike unit normal vector for M is presented as

$$\boldsymbol{\Gamma}(u,\theta) = \frac{-(\sigma\cos\theta + \eta\sin\theta)\boldsymbol{e}_1 - (r\cos\theta + \delta)(\cos\theta \boldsymbol{e}_2 + \sin\theta \boldsymbol{e}_3)}{\sqrt{-(\sigma\cos\theta + \eta\sin\theta)^2 + (r\cos\theta + \delta)^2}}. \tag{12}$$

By a straightforward calculation, we find

$$\begin{array}{c} \boldsymbol{P}_{\theta\theta} = -r(\cos\theta \boldsymbol{e}_2 + \sin\theta \boldsymbol{e}_3), \\ \boldsymbol{P}_{u\theta} = -r(\sin\theta \boldsymbol{e}_1 + \gamma\cos\theta \boldsymbol{e}_2 + \gamma\sin\theta \boldsymbol{e}_3), \\ \boldsymbol{P}_{uu} = (\delta' - \sigma)\boldsymbol{e}_1 + (\sigma' + r\cos\theta + \alpha)\boldsymbol{e}_2 + (\eta' + \sigma\gamma)\boldsymbol{e}_3 + \gamma \boldsymbol{P}_{\theta u}. \end{array} \tag{13}$$

Then, we have

$$\begin{aligned} h_{11} &= \left\{ \frac{\begin{array}{c}(r\cos\theta + \delta)[r\gamma - (\eta' + \sigma\gamma)\sin\theta - (\delta + r\cos\theta + \sigma')\cos\theta] \\ +(\alpha' - \sigma - r\gamma\sin\theta)(\eta\sin\theta + \sigma\cos\theta)\end{array}}{\sqrt{-(\sigma\cos\theta + \eta\sin\theta)^2 + (\delta + r\cos\theta)^2}} \right\}, \\ h_{12} &= \frac{r[-(\sigma\cos\theta + \eta\sin\theta)\sin\theta + \gamma(\delta + r\cos\theta)]}{\sqrt{-(\sigma\cos\theta + \eta\sin\theta)^2 + (\delta + r\cos\theta)^2}}, \\ h_{22} &= \frac{r(\delta + r\cos\theta)}{\sqrt{-(\sigma\cos\theta + \eta\sin\theta)^2 + (\delta + r\cos\theta)^2}}. \end{aligned} \tag{14}$$

The following definition is helpful:

Definition 2. *Assume M is the timelike circular surface with Equation (8). Therefore, at $u \in I \subseteq \mathbb{R}$, the following holds:*

(1) *M is named a timelike canal (tubular) surface in the case where the spine curve is perpendicular to the circular plane such that $\boldsymbol{\alpha}'(u)$, $\boldsymbol{e}_1(u)$, $\boldsymbol{e}_2(u)$ and $\boldsymbol{e}_3(u)$ satisfy*

$$\delta(u) =< \boldsymbol{e}_1, \boldsymbol{\alpha}' >\neq 0, \text{ and } < \boldsymbol{e}_2, \boldsymbol{\alpha}' >=< \boldsymbol{e}_3, \boldsymbol{\alpha}' >= 0 \Leftrightarrow \sigma(s) = \eta(s) = 0. \tag{15}$$

(2) *M is named a timelike roller coaster (or tangent) surface in the case where the spine curve is a tangent to the circular plane such that $\boldsymbol{\alpha}'(u)$, $\boldsymbol{e}_1(u)$, $\boldsymbol{e}_2(u)$ and $\boldsymbol{e}_3(u)$ satisfy*

$$\delta(u) =< \boldsymbol{e}_1, \boldsymbol{\alpha}' >= 0, \text{ and } \sigma(u) =< \boldsymbol{e}_2, \boldsymbol{\alpha}' >= 0 \text{ or } \eta(u) =< \boldsymbol{e}_3, \boldsymbol{\alpha}' >= 0. \tag{16}$$

A thorough treatment on timelike roller coaster surfaces will be given latter.

3.1. Striction Curves

As we know, the lines are the simplest examples of curves, and circles with a stationary radius give other simple examples of curves. Ruled surfaces are formed by a family of lines, and circular surfaces are formed by a set of circles with a stationary radius. Ruled surfaces have striction curves, and circular surfaces have spine curves. As a result, it is normal to investigate circular surfaces as an analogy with the ruled surfaces. Thus, for the timelike circular surface M, the curve

$$\boldsymbol{\zeta}(u) = \boldsymbol{\alpha}(u) + r(\cos\theta(u)\boldsymbol{e}_2(u) + \sin\theta(u)\boldsymbol{e}_3(u)), \tag{17}$$

is the striction curve if $\boldsymbol{\zeta}(u)$ ensures

$$< \boldsymbol{\zeta}', \cos\theta(u)\boldsymbol{e}_2(u) + \sin\theta(u)\boldsymbol{e}_3(u) >= 0.$$

This is equivalent to

$$\sigma(u)\cos\theta(u) + \eta(u)\sin\theta(u) = 0. \tag{18}$$

From Equation (18), it follows that striction points only exist when

$$\sin\theta(u) = \mp\frac{\sigma(u)}{\sqrt{\eta^2(u) + \sigma^2(u)}}, \text{ and } \cos\theta(u) = \pm\frac{\eta(u)}{\sqrt{\eta^2(u) + \sigma^2(u)}}. \tag{19}$$

Hence, two striction curves exist and are represented by

$$\left.\begin{aligned} \boldsymbol{\zeta}_1(u) &= \boldsymbol{\alpha}(u) + \tfrac{r}{\sqrt{\eta^2(u)+\sigma^2(u)}}(\eta(u)\boldsymbol{e}_2(u) - \sigma(u)\boldsymbol{e}_3(u)), \\ \boldsymbol{\zeta}_2(u) &= \boldsymbol{\alpha}(u) + \tfrac{r}{\sqrt{\eta^2(u)+\sigma^2(u)}}(-\eta(u)\boldsymbol{e}_2(u) + \sigma(u)\boldsymbol{e}_3(u)). \end{aligned}\right\} \tag{20}$$

In light of Equations (15) and (20), all curves on the timelike canal surface transverse to the generating circles ensure the condition of the striction curves; that is, $\boldsymbol{\zeta}_1(u) = \boldsymbol{\zeta}_2(u) = \boldsymbol{\alpha}(u)$. As a result, the sets of timelike canal surfaces are an analogous class to the sets of Lorentzian cylindrical surfaces:

Proposition 1. *Any non-canal timelike circular surface has two striction curves and intersects with every generating circle. Lorentzian circles are antipodal points to each other.*

3.2. Curvature Lines and Singularities

Here, we consider timelike circular surfaces whose generating circles are curvature lines, except for umbilical points or singular points. Using Equations (10) and (12), it is clear that all generating circles are curvature lines if

$$\boldsymbol{\Gamma}_{\vartheta}\|\boldsymbol{P}_{\vartheta} \Leftrightarrow 2r\|\boldsymbol{P}_u \times \boldsymbol{P}_{\theta}\|^2(r\eta + \delta\eta\cos\theta - \delta\sigma\sin\theta) = 0. \tag{21}$$

We will now research this situation in detail. In case $r = 0$, then M cannot be generated. (In reality, we have assumed $r > 0$.) In addition, if $\|\boldsymbol{P}_u \times \boldsymbol{P}_{\theta}\| = 0$, then the surface M is not regular. As stated in the assumption of M being regular, we find

$$r\eta + \delta(\eta\cos\theta - \sigma\sin\theta) = 0, \tag{22}$$

for all θ. Then, we have the following:

Case (1) When $\delta = \sigma = \eta = 0$, then $\boldsymbol{\alpha}' = \mathbf{0}$; that is, the spine curve is a fixed point. This means that the timelike circular surface is a Lorentzian sphere with a radius r. Namely, $M = \{\boldsymbol{P} \in \mathbb{E}_1^3 \mid \|\boldsymbol{P} - \boldsymbol{\alpha}\|^2 = r^2\}$.

Case (2) When $\sigma = \eta = 0$, the spine curve is orthogonal to the spacelike circular plane; that is, $\boldsymbol{\alpha}'$ is parallel to $\boldsymbol{e}_1$. Therefore, the timelike circular surface turns into a timelike canal surface with a timelike spine curve.

Case (3) When $\delta = \eta = 0$, the tangent vector $\boldsymbol{\alpha}'$ is parallel to $\boldsymbol{e}_2$. Hence, the tangent vector of the spine curve lies at the spacelike circle plane for all points of M. Specifically, $\boldsymbol{\alpha}' = \sigma\boldsymbol{e}_2$. When σ is constant, consequently, we have

$$\boldsymbol{\alpha} = \boldsymbol{\alpha}_0 + \sigma\boldsymbol{e}_1, \tag{23}$$

where $\boldsymbol{\alpha}_0$ is a constant vector. However, using Eqations (8) and (23) leads to

$$\|\boldsymbol{P} - \boldsymbol{\alpha}_0\|^2 = -\sigma^2 + r^2 > 0, \tag{24}$$

This implies that all the circle points lie on a Lorentzian sphere of a radius $r > |\sigma|$, with $\boldsymbol{\alpha}_0$ being its center point in $\mathbb{E}_1^3$.

After the above explanation we give the following theorem:

Theorem 1. *In the Minkowski 3-space $\mathbb{E}_1^3$, aside from the general timelike circular surfaces, there are two sets of timelike circular surfaces whose generating circles are curvature lines. These two sets are the timelike roller coaster surfaces and the Lorentzian spheres with a radius less than that of the generating circles.*

Singularities are essential for aspects of timelike circular surfaces and are defined as follows. In Equations (6)–(9), it is shown that M has a singular point at (s, θ) if

$$< \boldsymbol{e}_1, \boldsymbol{\alpha}' + r\cos\theta\boldsymbol{e}_2{}' + r\sin\theta\boldsymbol{e}_3{}' >= 0, \text{ and } < \boldsymbol{\alpha}', r\cos\theta\boldsymbol{e}_2 + r\sin\theta\boldsymbol{e}_3 >= 0,$$

This yields two (linearly dependent) equations:

$$\delta + r\cos\theta = 0, \text{and } \sigma\cos\theta + \eta\sin\theta = 0. \tag{25}$$

The singular points are discussed as follows:

Case (1) This exists when $\delta + r\cos\theta = 0$. If $\sigma \neq 0$ and $\eta \neq 0$, then the singular points are located at $\theta = \sin^{-1}(\sigma\delta/\eta r)$ and $\theta = \pi + \sin^{-1}(\sigma\delta/\eta r)$. If $\delta \neq 0$ and $\eta = 0$, then the singular points are located at $\theta = \pm\cos^{-1}(\delta/r)$. If $\delta = 0$, for a timelike circular surface to have singular points, it is necessary that $\cos\theta = 0 = \eta$. Therefore, there are two singular points on the generating circle, located at $\theta = \pm\pi/2$.

Case (2) This exists if $\theta = -\tan^{-1}(\sigma/\eta)$. In the case of a timelike circular surface having singular points, it is necessary that $\delta - r\cos\theta = 0$. Since $|\cos\theta| \leq 1$, we can say that the singularities are only located when $\theta = \pi/2$ and $3\pi/2$. Thus, there are two singular points on each generating circle. Adding these two sets of singular points results in two curves (striction curves) that contain all the singular points of a timelike circular surface. Then, the striction curves form a timelike circular surface.

Under the above notations, it might be said that the geometrical properties of timelike circular surfaces are analogues with those of developable ruled surfaces. Lorentzian spheres correspond to cones, timelike canal surfaces to cylinders and timelike roller coaster surfaces to tangent developable surfaces. Hence, the following corollary can be given:

Corollary 1. *Suppose M is a timelike circular surface which has generating circles as curvature lines, except at umbilical points or singular points. Therefore, M is a part of a Lorentzian sphere, a timelike canal surface and a timelike roller coaster surface.*

3.3. Timelike Canal (Tubular) Surfaces

Here, we check and construct a timelike canal surface ($\sigma = \eta = 0 = 0$) whose parametric curves are curvature lines. Then, using Eqations (11) and (14), we consequently have $g_{12} = h_{12} = 0 \Leftrightarrow \gamma = 0$. If we use this in Equation (6), we obtain the following ODE:

$$\boldsymbol{e}_1'' - \boldsymbol{e}_1 = \mathbf{0}.$$

From this equation, the spherical curve $\boldsymbol{e}_1(u)$ can be represented as

$$\boldsymbol{e}_1(u) = (\sinh u, 0, \cosh u), \tag{26}$$

which is a timelike unit vector. Clearly, we have

$$\boldsymbol{e}_2(u) = (\cosh u, 0, \sinh u),\ \boldsymbol{e}_3(u) = (0, 1, 0). \tag{27}$$

Assuming an integral with zero integration constants yields

$$\boldsymbol{\alpha}(u) = \int_0^u \delta(u)(\sinh u, 0, \cosh u)du.$$

Let us choose $\delta(u) = u$. Therefore, we have

$$\boldsymbol{\alpha}(u) = (u\cosh u - \sinh u, 0, u\sinh u - \cosh u). \tag{28}$$

It is clear that $\boldsymbol{\alpha}(u)$ has a singular point (cusp) at $u = 0$ (Figure 2). Thus, the timelike canal surface M with the timelike spine curve $\boldsymbol{\alpha}(u)$ is given by

$$M : \boldsymbol{P}(u,\theta) = (u\cosh u - \cosh u + r\cos\theta\cosh u, r\sin\theta, u\sinh u - \sinh u + r\cos\theta\sinh u).$$

For $r = 0.3$, with $0 \leq \theta \leq 2\pi$ and $-3 \leq u \leq 3$, the surface is illustrated in Figure 3.

We now give an example regarding singularity and the striction curve of a non-canal timelike circular surface:

Example 1. *A non-canal timelike circular surface can be defined as follows. Take the Blaschke frame as shown in Equation (27) and $\gamma(u) = \delta(u) = \eta(u) = 1$. Then, it is easy to derive*

$$\boldsymbol{\alpha}(u) = (\cosh u + \sinh u, u, \sinh u + \cosh u).$$

which shows that $\boldsymbol{\alpha}(u)$ has no singular point. Then, according to Equation (20), the striction curves are

$$\left.\begin{array}{l}\zeta_1(u) = (\cosh u + \sinh u, u, \sinh u + \cosh u) + \frac{r}{\sqrt{2}}(\cosh u, -1, \sinh u), \\ \zeta_2(u) = (\cosh u + \sinh u, u, \sinh u + \cosh u) + \frac{r}{\sqrt{2}}(-\cosh u, 1, -\sinh u).\end{array}\right\}$$

The timelike circular surface M with the spine curve $\boldsymbol{\alpha}(u)$ is then given by

$$M : \boldsymbol{P}(u,\theta) = (\sinh u + (1 + r\cos\theta)\cosh u, u + r\sin\theta, \cosh u + (1 + r\cos\theta)\sinh u),$$

which has different singularities appear on the striction curves (green), where $r = 1$, with $0 \leq \theta \leq 2\pi$ and $-1.5 \leq u \leq 1.5$ (Figure 4).

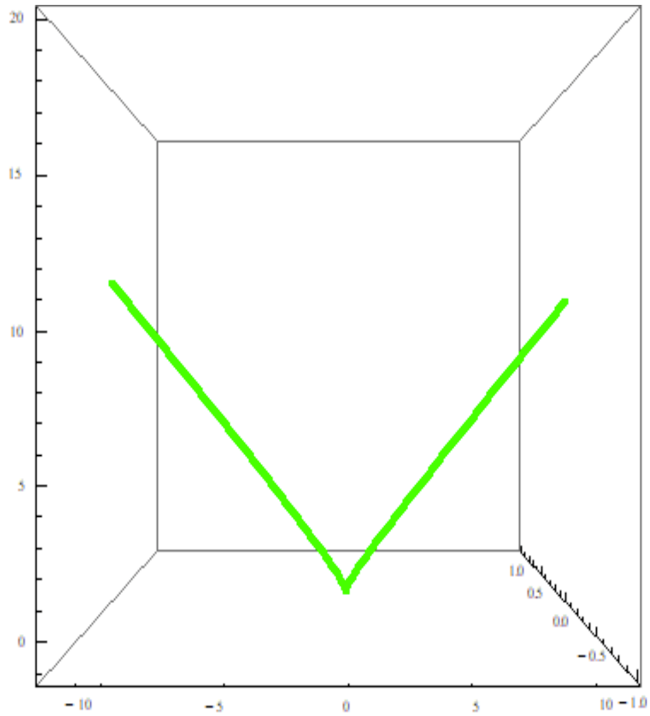

Figure 2. $\boldsymbol{\alpha}(u)$ has a cusp at $u = 0$.

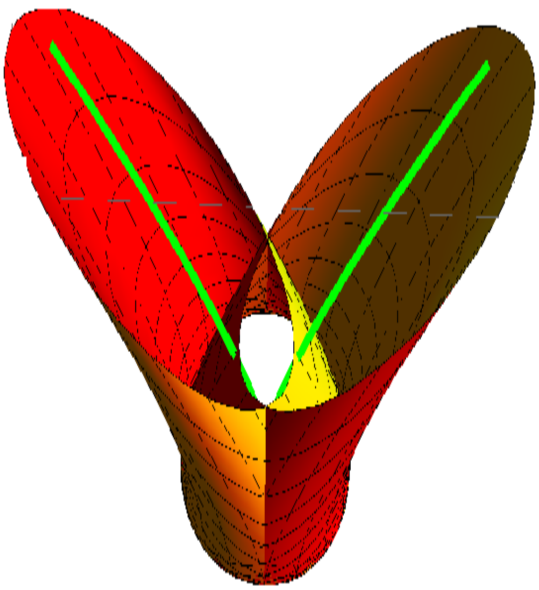

Figure 3. M has different singular points.

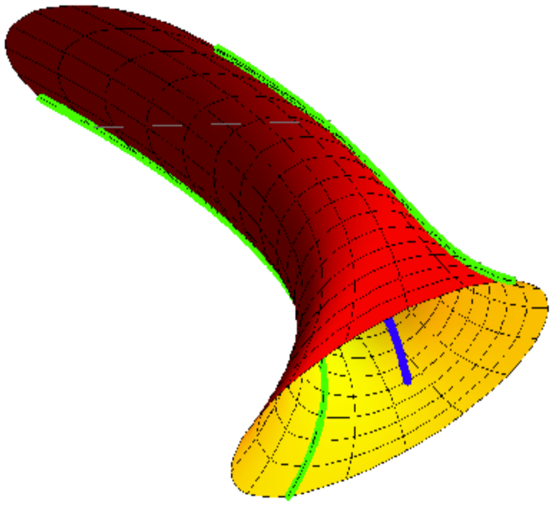

Figure 4. *M* has different singular points along the striction curves.

3.4. Timelike Canal (Tubular) Surface

We now derive a parametric representation of a timelike canal (tubular) surface with a timelike spine curve. Consider s to be the arc length parameter of $\boldsymbol{\alpha}$ and $\{\boldsymbol{T}(s), \boldsymbol{N}(s), \boldsymbol{B}(s)\}$ to be its Serret–Frenet frame. Then, we have

$$\boldsymbol{T}(s) = \frac{\boldsymbol{\alpha}'}{\|\boldsymbol{\alpha}'\|} = \boldsymbol{e}_1,\ \boldsymbol{N}(s) = \frac{d\boldsymbol{T}}{ds}\left\|\frac{d\boldsymbol{T}}{ds}\right\|^{-1} = \boldsymbol{e}_2,\ \boldsymbol{B}(s) = \boldsymbol{e}_3, \tag{29}$$

and

$$\begin{pmatrix} \boldsymbol{T}' \\ \boldsymbol{N}' \\ \boldsymbol{B}' \end{pmatrix} = \begin{pmatrix} 0 & \kappa & 0 \\ \kappa & 0 & \tau \\ 0 & -\tau & 0 \end{pmatrix} \begin{pmatrix} \boldsymbol{T} \\ \boldsymbol{N} \\ \boldsymbol{B} \end{pmatrix},\ \left({}' = \frac{d}{ds}\right)$$

where $\kappa(s)$ and $\tau(s)$ define the natural curvature and torsion:

$$\kappa(s) = \frac{1}{|\delta|},\ \tau(s) = \frac{\gamma}{\delta}, \text{ with } \delta \neq 0.$$

Notably, as long as $\boldsymbol{T}(s)$ is perpendicular to the circle planes at all points of the spine curve, the canal surface can be defined as

$$M : \boldsymbol{P}(s,\theta) = \boldsymbol{\alpha}(s) + r(\cos\theta\boldsymbol{N} + \sin\theta\boldsymbol{B}),\ s \in I,\ \theta \in \mathbb{R}.$$

The $\boldsymbol{P}'s$ tangent vectors are

$$\boldsymbol{P}_s = \mu\boldsymbol{T} + \tau\boldsymbol{P}_\theta, \text{ and } \boldsymbol{P}_\theta = r(-\sin\theta\boldsymbol{N} + \cos\theta\boldsymbol{B}),$$

where $\mu = 1 + r\kappa\cos\theta$ such that

$$g_{11} = -\mu^2 + r^2\tau^2,\ g_{12} = r^2\tau,\ g_{22} = r^2,$$

and

$$\boldsymbol{\Gamma}(s,\theta) = \cos\theta\boldsymbol{N} + \sin\theta\boldsymbol{B}.$$

Then, we have

$$\begin{gathered} \boldsymbol{P}_{\theta\theta} = -r(\cos\theta\boldsymbol{N} + \sin\theta\boldsymbol{B}), \\ \boldsymbol{P}_{s\theta} = -r\kappa\sin\theta\boldsymbol{T} - r\tau(\cos\theta\boldsymbol{N} + \sin\theta\boldsymbol{B}), \\ \boldsymbol{P}_{ss} = r(\kappa'\cos\theta - \kappa\tau\sin\theta)\boldsymbol{T} + r\left[\mu\kappa - r\left(\tau'\sin\theta + \tau^2\cos\theta\right)\right]\boldsymbol{N} \\ +r\left(\tau'\cos\theta - \tau^2\sin\theta\right)\boldsymbol{B}. \end{gathered}$$

Therefore, we can write

$$h_{11} = -r\tau^2 + \mu\kappa\cos\theta,\ h_{12} = -r\tau,\ h_{22} = -r.$$

Hence, the Gaussian and mean curvatures can be calculated as

$$K(s,\theta) = \frac{\kappa\cos\theta}{\mu r}, \text{ and } H(s,\theta) = \frac{1}{2}\left(\frac{1}{r} + rK(s,\theta)\right).$$

On the other hand, because every Lorentzian generating circle is a curvature line, the value of one principal curvature is

$$\chi_1(s,\theta) := \|\boldsymbol{P}_\theta \times \boldsymbol{P}_{\theta\theta}\| \|\boldsymbol{P}_\theta\|^{-3} = \frac{1}{r}.$$

The principle direction of χ_1 points in the direction of the Lorentzian generating circle, and this curvature is constant:

Corollary 2. *The principal curvature of a timelike canal surface is constant along all generating Lorentzian circles.*

Example 2. *Let $\boldsymbol{\alpha}(s) = (\sin\frac{s}{2}, \cos\frac{s}{2}, \frac{\sqrt{5}}{2}s)$, $-2\pi \leq s \leq 2\pi$ be a unit speed timelike helix. Clearly, we have*

$$\left.\begin{array}{l} \boldsymbol{T}(s) = (\frac{1}{2}\cos\frac{s}{2}, -\frac{1}{2}\sin\frac{s}{2}, \frac{\sqrt{5}}{2}), \\ \boldsymbol{N}(s) = (-\sin\frac{s}{2}, -\cos\frac{s}{2}, 0), \\ \boldsymbol{B}(s) = (\frac{\sqrt{5}}{2}\cos\frac{s}{2}, -\frac{\sqrt{5}}{2}\sin\frac{s}{2}, \frac{1}{2}). \end{array}\right\}$$

Hence, we construct the timelike canal surface as follows:

$$\boldsymbol{P}(s,\theta) = (\sin\frac{s}{2}, \cos\frac{s}{2}, \frac{\sqrt{5}}{2}s) + r(0, \cos\theta, \sin\theta)\begin{pmatrix} \frac{1}{2}\cos\frac{s}{2} & -\frac{1}{2}\sin\frac{s}{2} & \frac{\sqrt{5}}{2} \\ -\sin\frac{s}{2} & -\cos\frac{s}{2} & 0 \\ \frac{\sqrt{5}}{2}\cos\frac{s}{2} & -\frac{\sqrt{5}}{2}\sin\frac{s}{2} & \frac{1}{2} \end{pmatrix}.$$

The spine curve has no singular points. Clearly, $\mathbf{P}(s,\theta)$ has different singularities with $r = 1$ and $0 \leq \theta \leq 2\pi$ (Figure 5).

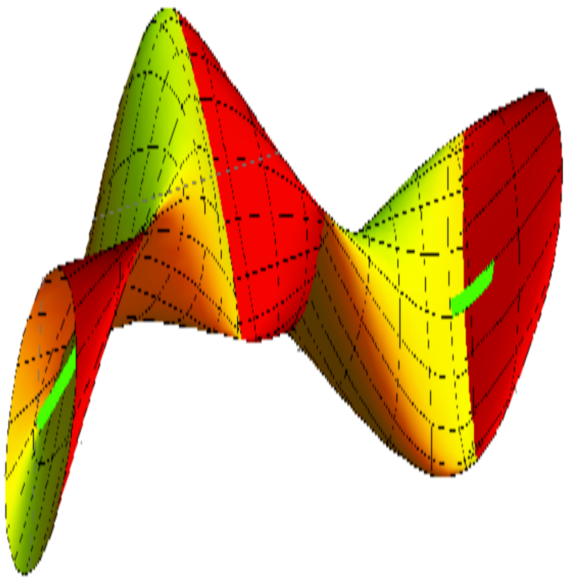

Figure 5. M has different singular points.

3.5. Timelike Roller Coaster Surfaces

Timelike roller coaster surfaces are considered to be those where the tangent vector of the spine curve $\boldsymbol{\alpha}$ lies in the spacelike circle plane at all points of $\boldsymbol{\alpha}$. This means that $\delta(u) = 0$, $\sigma(u)$ and $\eta(u)$ do not equal zero simultaneously. Through this work, we will only assume that $\delta(u) = \eta(u) = 0$ and $\sigma(u) \neq 0$. If so, such a surface is called a timelike roller coaster surface with a spacelike spine curve; that is, $\boldsymbol{\alpha}'(u) = \sigma(u)\boldsymbol{e}_2$. From Equation (19), it follows that $\theta = \pi/2$ and $3\pi/2$. Hence, the equation of the striction curves is

$$\boldsymbol{\zeta}_{1,2}(u) = \boldsymbol{\alpha}(u) \pm r\boldsymbol{e}_3(u), \tag{30}$$

which contains all the singular points. Therefore, striction curves form a timelike roller coaster surface with a spacelike spine curve. The curvature and torsion may be derived, depending on $\sigma(u)$ and $\gamma(u)$, as follows:

$$\begin{aligned} \kappa_1(u) &= \frac{1}{\sigma - r\gamma}\sqrt{-1+\gamma^2},\ \tau_1(u) = \frac{\gamma'}{(-1+\gamma^2)(\sigma - r\gamma)}, \\ \kappa_2(u) &= \frac{1}{\sigma + r\gamma}\sqrt{-1+\gamma^2},\ \tau_2(u) = \frac{\gamma'}{(-1+\gamma^2)(\sigma + r\gamma)}. \end{aligned} \tag{31}$$

Thus, if γ is a constant, then the torsions τ_i are zero simultaneously; that is, the striction curves are planar spacelike curves. Moreover, the Gaussian and mean curvatures at a regular point can be written as

$$\begin{aligned} K(u,\theta) &= \frac{1}{r^2 - \sigma^2} + \frac{r\sigma'}{(r^2 - \sigma^2)^2 \cos\theta}, \\ H(u,\theta) &= \frac{\sigma'}{2r\left(\sqrt{r^2 - \sigma^2}\right)^3 \cos\theta} + \frac{1}{\sqrt{r^2 - \sigma^2}}. \end{aligned} \tag{32}$$

It is a noteworthy fact that concepts such as both Gaussian curvature and principal curvatures, whose definition makes fundamental use of the location of a surface in a space, do not rely on the geodesic curvature of $\boldsymbol{e}_1 \in \mathbb{H}^2_+$ but only on σ and θ. Hence, the following conclusions can be given:

Theorem 2. *If a set of timelike roller coaster surfaces has an equal radius and scalar σ, and its derivative is σ', then the Gaussian as well as the mean curvatures at corresponding points will be equal to each other at the corresponding point. Moreover, their values are independent of the geodesic curvature of the hyperbolic spherical image curve $\boldsymbol{e}_1 \in \mathbb{H}^2_+$.*

Furthermore, to study the kinematic-geometric possessions of the timelike roller coaster surface, the Serret–Frenet of the spine curve $\boldsymbol{\alpha}(u)$ is necessary to build. Therefore, assume v be the arc length of the spacelike spine curve $\boldsymbol{\alpha}(u)$ and $\sigma(u) > 0$ at all $u \in I \subseteq \mathbb{R}$, where the Serret–Frenet frame of the spine curve can be presented as

$$\boldsymbol{t}(v) = \frac{\boldsymbol{\alpha}'}{\|\boldsymbol{\alpha}'\|} = \boldsymbol{e}_2,\ \boldsymbol{n}(v) = \frac{\boldsymbol{t}'}{\|\boldsymbol{t}'\|} = \frac{\boldsymbol{e}_1 + \gamma\boldsymbol{e}_3}{\sqrt{\gamma^2 - 1}},\ \boldsymbol{b}(v) = \frac{\gamma\boldsymbol{e}_1 + \boldsymbol{e}_3}{\sqrt{\gamma^2 - 1}}.$$

By letting $\cosh\varphi = \frac{\gamma}{\sqrt{\gamma^2-1}}$, $\sinh\varphi = \frac{1}{\sqrt{\gamma^2-1}}$, $|\gamma| > 1$, it follows that

$$\begin{pmatrix} \boldsymbol{t} \\ \boldsymbol{n} \\ \boldsymbol{b} \end{pmatrix} = \begin{pmatrix} 0 & 1 & 0 \\ \sinh\varphi & 0 & \cosh\varphi \\ \cosh\varphi & 0 & \sinh\varphi \end{pmatrix} \begin{pmatrix} \boldsymbol{e}_1 \\ \boldsymbol{e}_2 \\ \boldsymbol{e}_3 \end{pmatrix}, \tag{33}$$

Thus, we have

$$\frac{d}{dv}\begin{pmatrix} \boldsymbol{t} \\ \boldsymbol{n} \\ \boldsymbol{b} \end{pmatrix} = \begin{pmatrix} 0 & \kappa(v) & 0 \\ -\kappa(v) & 0 & \tau(v) \\ 0 & \tau(v) & 0 \end{pmatrix}\begin{pmatrix} \boldsymbol{t} \\ \boldsymbol{n} \\ \boldsymbol{b} \end{pmatrix},$$

where

$$\begin{aligned} \kappa(v) &= \frac{1}{\sigma}\sqrt{\gamma^2-1},\ \tau(v) - \frac{d\varphi}{dv} = 0, \\ \frac{d\varphi}{dv} &= \frac{\gamma'}{\sigma(\gamma^2-1)},\ \varphi(v) = -\int_0^v \tau dv + \varphi_0. \end{aligned} \tag{34}$$

The timelike roller coaster surface can be presented as

$$M : \boldsymbol{P}(s,\theta) = \boldsymbol{\alpha} + r[\cos\theta \boldsymbol{t} + \sin\theta(\cosh\varphi \boldsymbol{n} - \sinh\varphi \boldsymbol{b})]. \tag{35}$$

Furthermore, the two striction curves are

$$\left.\begin{aligned} \boldsymbol{\zeta}_1(v) = \boldsymbol{\alpha}(v) - r(\cosh\varphi \boldsymbol{n}(v) - \sinh\varphi \boldsymbol{b}(v)), \\ \boldsymbol{\zeta}_2(v) = \boldsymbol{\alpha}(v) + r(\cosh\varphi \boldsymbol{n}(v) - \sinh\varphi \boldsymbol{b}(v)). \end{aligned}\right\} \tag{36}$$

As in the previous equations, we not only prove the existence of the timelike roller coaster, but we also give the specified expression of the surface. This is very significant in practical application.

A surface with zero Gaussian curvature is called a flat surface. Clearly, M is flat if $K(u,\theta) = (r^2-\sigma^2)^2\cos\theta + r\sigma' = 0$. Thus, for every $\theta \in I \subseteq \mathbb{R}$, we have

$$\frac{\partial^2 K(u,\theta))}{\partial^2\theta} + K(u,\theta) = 0 \Leftrightarrow \sigma'(u) = 0. \tag{37}$$

Using Equations (32) and (34), the indication of $\sigma'(u)$ in terms of the Serret–Frenet invariants is

$$\sigma'(u) = 0 \Leftrightarrow \kappa(v)\tau(v)\cosh\varphi(v) + \frac{d\kappa}{dv}\sinh\varphi(v) = 0.$$

Therefore, in a neighborhood of every point on M with $\kappa(v) \neq 0$, we have $\frac{d\kappa(v)}{dv} = \tau(v) = 0$. Therefore, a timelike roller coaster surface whose Gaussian curvature vanishes identically is a part of the timelike plane. In the same method, we find that M is a timelike minimal flat surface. Hence, we state the following:

Corollary 3. *All the flat (minimal) timelike roller coaster surfaces are subsets of Lorentzian planes.*

Example 3. *Take the case of a parametric spacelike circular helix, such as*

$$\boldsymbol{\alpha}(v) = (a\cos v, a\sin v, bv),\ a > 0,\ \ b \neq 0,\ a^2 - b^2 = 1,\ 0 \leq v \leq \pi.$$

With normal computation, we have

$$\boldsymbol{t}(v) = (-a\sin v, a\cos v, b),\ \boldsymbol{n}(v) = (\cos v, \sin v, 0),\ \boldsymbol{b}(v) = (-b\sin v, b\cos v, a).$$

Clearly, if $\tau = b$, then $\varphi(v) = bv + \varphi_0$. In the case of $\varphi_0 = 0$, we have $\varphi(v) = bv$. For $a = 2$ and $r = 1$, the corresponding timelike roller coaster surface with the spine curve $\boldsymbol{\alpha}(v)$ (blue) is shown in Figure 6. Singularities appear on the striction curves (green).

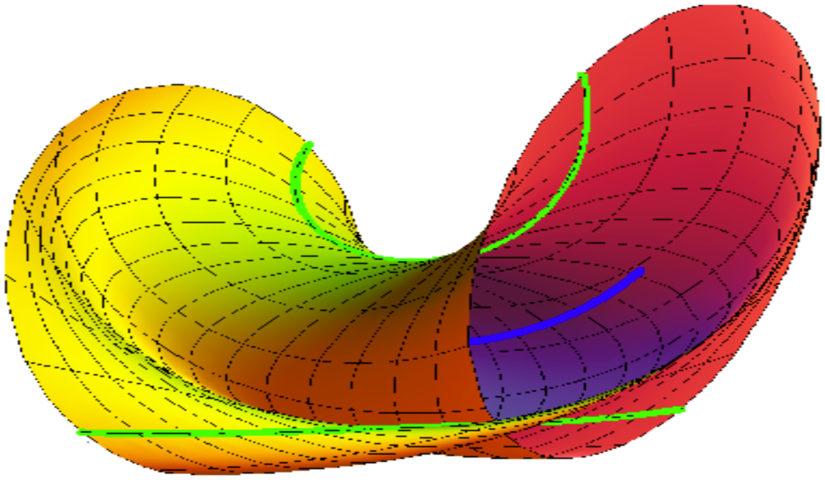

Figure 6. Timelike roller coaster surface with its spine and striction curves.

4. Conclusions

This work investigates the smooth one-parameter family of standard Lorentzian circles with a fixed radius. A similar surface, named a timelike circular surface, has a fixed radius. Then, several corresponding properties of timelike circular surfaces with ruled surfaces were obtained. Through the differential operation of the frame, the geometric properties of the timelike circular surface are explained, and their geometric meanings are presented. Additionally, the conditions for timelike roller coaster surfaces to be flat or minimal surfaces are obtained. Finally, some illustrative examples were presented. Furthermore, interdisciplinary research can provide valuable new insights, but synthesizing articles across disciplines with highly varied standards, formats, terminology, and methods required an adapted approach. Recently, many interesting papers have been written related to symmetry, molecular cluster geometry analysis, submanifold theory, singularity theory, eigenproblems, etc. [17–53]. In future works, we plan to study the timelike circular surfaces and singularities for different queries and further improve the results in this paper, combined with the technics and results in [17–53]. We intend to perform the implementation of those results and explore new methods to find more results and theorems related to the symmetric properties of this topic in our following papers.

Author Contributions: Conceptualization, Y.L., F.M. and R.A.A.-B.; methodology, Y.L., F.M. and R.A.A.-B.; investigation, Y.L., F.M. and R.A.A.-B.; writing—original draft preparation, Y.L., F.M. and R.A.A.-B.; writing—review and editing, Y.L., F.M. and R.A.A.-B. All authors have read and agreed to the published version of the manuscript.

Funding: This research was funded by the National Natural Science Foundation of China (grant No. 12101168), Zhejiang Provincial Natural Science Foundation of China (grant No. LQ22A010014) and Princess Nourah bint Abdulrahman University Researchers Supporting Project number (PNURSP2022R27) of Princess Nourah bint Abdulrahman University in Riyadh, Saudi Arabia.

Institutional Review Board Statement: Not applicable.

Informed Consent Statement: Not applicable.

Data Availability Statement: Not applicable.

Acknowledgments: We gratefully acknowledge the constructive comments from the editor and the anonymous referees and Princess Nourah bint Abdulrahman University Researchers Supporting Project number (PNURSP2022R27) of Princess Nourah bint Abdulrahman University in Riyadh, Saudi Arabia.

Conflicts of Interest: The authors declare no conflict of interest.

References

1. Izumiya, S.; Takeuchi, N. Singularities of ruled surfaces in $\mathbb{E}^3$. In *Mathematical Proceedings of the Cambridge Philosophical Society*; Cambridge University Press: Cambridge, UK, 2001; Volume 130.
2. Izumiya, S.; Takeuchi, N. Geometry of ruled surfaces. In *Applicable Mathematics in the Golden Age*; Narosa Publishing House: New Delhi, India, 2003; pp. 305–338.
3. Izumiya, S. Special curves and ruled surfaces. *Contrib. Algebra Geom.* **2003**, *44*, 203–212.
4. Blum, R. Circles on surfaces in the Euclidean 3-space. In *Geometry and Differential Geometry*; Lecture Notes in Mathematics; Springer: Berlin/Heidelberg, Germany, 1980; Volume 792, pp. 213–221.
5. Xu, Z.; Feng, R.; Sun, J. Analytic and algebraic properties of canal surfaces. *J. Comput. Appl. Math.* **2006**, *195*, 220–228. [CrossRef]
6. Cui, L.; Wang, D.L.; Dai, J.S. Kinematic geometry of circular surfaces with a fixed radius based on Euclidean invariants. *ASME J. Mech.* **2009**, *131*, 101009.
7. Izumiya, S.; Saji, K.; Takeuchi, N. Circular surfaces. *Adv. Geom.* **2007**, *7*, 295–313. [CrossRef]
8. Izumiya, S.; Saji, K.; Takeuchi, N. Great circular surfaces in the three-sphere. *Differ. Geom. Appl.* **2011**, *29*, 409–425. [CrossRef]
9. Gorjanc, S.; Jurkin, E. Circular surfaces CS(α, p). *Filomat* **2015**, *29*, 725–737 [CrossRef]
10. Abdel-Baky, R.A.; Unluturk, Y. On the curvatures of spacelike circular surfaces. *Kuwait J. Sci.* **2016**, *43*, 50–58.
11. Tuncer, O.; Canakcı, Z.; Gok, I.; Yaylı, Y. Circular surfaces with split quaternionic representations in Minkowski 3-space. *Adv. Appl. Clifford Algebr.* **2018**, *28*, 63. [CrossRef]
12. Alluhaibi, N. Circular surfaces and singularities in Euclidean 3-space E^3. *AIMS Math.* **2022**, *7*, 12671–12688. [CrossRef]
13. Abdel-Baky, R.; Alluhaibi, N.; Ali, A.; Mofarreh, F. A study on timelike circular surfaces in Minkowski 3-space. *Int. J. Geom. Methods Mod. Phys.* **2020**, *17*, 2050074. [CrossRef]
14. O'Neil, B. *Semi-Riemannian Geometry with Applications to Relativity*; Academic Press: New York, NY, USA, 1983.
15. Mc-Nertney, L.V. One-Parameter Families of Surfaces with Constant Curvature in Lorentz Three-Space. Ph.D. Thesis, Brown University, Providence, RI, USA, 1980.
16. Walrave, J. Curves and Surfaces in Minkowski Space. Ph.D. Thesis, K.U. Leuven, Faculty of Science, Leuven, Belgium, 1995.
17. Sharma, J.R.; Kumar, S.; Jäntschi, L. On a class of optimal fourth order multiple root solvers without using derivatives. *Symmetry* **2019**, *11*, 1452. [CrossRef]
18. Joita, D.M.; Tomescu, M.A.; Bàlint, D.; Jäntschi, L. An Application of the Eigenproblem for Biochemical Similarity. *Symmetry* **2021**, *13*, 1849. [CrossRef]
19. Jäntschi, L. Introducing Structural Symmetry and Asymmetry Implications in Development of Recent Pharmacy and Medicine. *Symmetry* **2022**, *14*, 1674. [CrossRef]
20. Jäntschi, L. Binomial Distributed Data Confidence Interval Calculation: Formulas, Algorithms and Examples. *Symmetry* **2022**, *14*, 1104. [CrossRef]
21. Jäntschi, L. Formulas, Algorithms and Examples for Binomial Distributed Data Confidence Interval Calculation: Excess Risk, Relative Risk and Odds Ratio. *Mathematics* **2021**, *9*, 2506. [CrossRef]
22. Donatella, B.; Jäntschi, L. Comparison of Molecular Geometry Optimization Methods Based on Molecular Descriptors. *Mathematics* **2021**, *9*, 2855.
23. Mihaela, T.; Jäntschi, L.; Doina, R. Figures of Graph Partitioning by Counting, Sequence and Layer Matrices. *Mathematics* **2021**, *9*, 1419.
24. Kumar, S.; Kumar, D.; Sharma, J.R.; Jäntschi, L. A Family of Derivative Free Optimal Fourth Order Methods for Computing Multiple Roots. *Symmetry* **2020**, *12*, 1969. [CrossRef]
25. Deepak, K.; Janak, R.; Jäntschi, L. A Novel Family of Efficient Weighted-Newton Multiple Root Iterations. *Symmetry* **2020**, *12*, 1494.
26. Janak, R.; Sunil, K.; Jäntschi, L. On Derivative Free Multiple-Root Finders with Optimal Fourth Order Convergence. *Mathematics* **2020**, *8*, 1091.
27. Jäntschi, L. Detecting Extreme Values with Order Statistics in Samples from Continuous Distributions. *Mathematics* **2020**, *8*, 216. [CrossRef]
28. Deepak, K.; Janak, R.; Jäntschi, L. Convergence Analysis and Complex Geometry of an Efficient Derivative-Free Iterative Method. *Mathematics* **2019**, *7*, 919.
29. Jäntschi, L.; Bolboacă, S.D. Conformational study of C_{24} cyclic polyyne clusters. *Int. J. Quantum Chem.* **2018**, *118*, 25614. [CrossRef]
30. Ünlütürk, Y.; Yilmaz, S. A new approach to timelike surfaces which contain inclined curves as geodesics. *Differ. Equ. Dyn. Syst.* **2019**, 1–8. [CrossRef]
31. Yang, Z.C.; Li, Y.; Erdoğdub, M.; Zhu, Y.S. Evolving evolutoids and pedaloids from viewpoints of envelope and singularity theory in Minkowski plane. *J. Geom. Phys.* **2022**, *176*, 104513. [CrossRef]
32. Li, Y.; Ganguly, D.; Dey, S.; Bhattacharyya, A. Conformal η-Ricci solitons within the framework of indefinite Kenmotsu manifolds. *AIMS Math.* **2022**, *7*, 5408–5430. [CrossRef]
33. Li, Y.; Abolarinwa, A.; Azami, S.; Ali, A. Yamabe constant evolution and monotonicity along the conformal Ricci flow. *AIMS Math.* **2022**, *7*, 12077–12090. [CrossRef]
34. Li, Y.; Khatri, M.; Singh, J.P.; Chaubey, S.K. Improved Chen's Inequalities for Submanifolds of Generalized Sasakian-Space-Forms. *Axioms* **2022**, *11*, 324. [CrossRef]
35. Li, Y.; Uçum, A.; İlarslan, K.; Camcı, Ç. A New Class of Bertrand Curves in Euclidean 4-Space. *Symmetry* **2022**, *14*, 1191. [CrossRef]

36. Li, Y.; Mofarreh, F.; Agrawal, R.P.; Ali, A. Reilly-type inequality for the Φ-Laplace operator on semislant submanifolds of Sasakian space forms. *J. Inequal. Appl.* **2022**, *2022*, 102. [CrossRef]
37. Li, Y.; Mofarreh, F.; Dey, S.; Roy, S.; Ali, A. General Relativistic Space-Time with η_1-Einstein Metrics. *Mathematics* **2022**, *10*, 2530. [CrossRef]
38. Li, Y.; Dey, S.; Pahan, S.; Ali, A. Geometry of conformal η-Ricci solitons and conformal η-Ricci almost solitons on Paracontact geometry. *Open Math.* **2022**, *20*, 574–589. [CrossRef]
39. Li, Y.; Şenyurt, S.; Özduran, A.; Canlı, D. The Characterizations of Parallel q-Equidistant Ruled Surfaces. *Symmetry* **2022**, *14*, 1879. [CrossRef]
40. Li, Y.; Haseeb, A.; Ali, M. LP-Kenmotsu manifolds admitting η-Ricci solitons and spacetime. *J. Math.* **2022**, *2022*, 6605127.
41. Antić, M.; Moruz, M.; Van, J. H-Umbilical Lagrangian Submanifolds of the Nearly Kähler $\mathbb{S}^3 \times \mathbb{S}^3$. *Mathematics* **2020**, *8*, 1427. [CrossRef]
42. Antić, M.; Djordje, K. Non-Existence of Real Hypersurfaces with Parallel Structure Jacobi Operator in $S^6(1)$. *Mathematics* **2022**, *10*, 2271. [CrossRef]
43. Antić, M. Characterization of Warped Product Lagrangian Submanifolds in $\mathbb{C}^n$. *Results Math.* **2022**, *77*, 106. [CrossRef]
44. Antić, M.; Vrancken, L. Conformally flat, minimal, Lagrangian submanifolds in complex space forms. *Sci. China Math.* **2022**, *65*, 1641–1660. [CrossRef]
45. Antić, M.; Hu, Z.; Moruz, M.; Vrancken, L. Surfaces of the nearly Kähler $\mathbb{S}^3 \times \mathbb{S}^3$ preserved by the almost product structure. *Math. Nachr.* **2021**, *294*, 2286–2301. [CrossRef]
46. Antić, M. A class of four-dimensional CR submanifolds in six dimensional nearly Kähler manifolds. *Math. Slovaca* **2018**, *68*, 1129–1140. [CrossRef]
47. Antić, M. A class of four dimensional CR submanifolds of the sphere $S^6(1)$. *J. Geom. Phys.* **2016**, *110*, 78–89. [CrossRef]
48. Ali, A.T. Non-lightlike constant angle ruled surfaces in Minkowski 3-space. *J. Geom. Phys.* **2020**, *157*, 103833. [CrossRef]
49. Ali, A.T. A constant angle ruled surfaces. *Int. J. Geom.* **2018**, *7*, 69–80.
50. Ali, A.T. Non-lightlike ruled surfaces with constant curvatures in Minkowski 3-space. *Int. J. Geom. Methods Mod. Phys.* **2018**, *15*, 1850068. [CrossRef]
51. Ali, A.T.; Hamdoon, F.M. Surfaces foliated by ellipses with constant Gaussian curvature in Euclidean 3-space. *Korean J. Math.* **2017**, *25*, 537–554.
52. Ali, A.T.; Abdel Aziz, H.S.; Sorour, A.H. On some geometric properties of quadric surfaces in Euclidean space. *Honam Math. J.* **2016**, *38*, 593–611. [CrossRef]
53. Ali, A.T.; Abdel Aziz, H.S.; Sorour, A.H. On curvatures and points of the translation surfaces in Euclidean 3-space. *J. Egyptian Math. Soc.* **2015**, *23*, 167–172. [CrossRef]